Implementation of XFEM in the study of gear crack propagation behaviour using the SIF on different moments

Fung Zen Hiung

Department of Mechanical Engineering,
Curtin University,
CDT 250 98009 Miri, Malaysia
Email: fungzenhiung@gmail.com

Haidar F. Al-Qrimli*

Department of Mechanical Engineering,
School of Engineering and Physical Sciences,
Heriot-Watt University,
62200 Putrajaya, Malaysia
Email: halqrimli@yahoo.com
Email: h.al-qrimli@hw.ac.uk
*Corresponding author

Kenobi Isima Morris

Faculty of Engineering,
University of Nottingham Malaysia Campus,
Jalan Broga, 43500 Semenyih,
Selangor, Malaysia
Email: kenobi.morris@nottingham.edu.my

Abstract: The application of gears, especially spur gear, is widely available in most engineering applications. Especially for high module steel spur gear, it is used extensively in heavy machineries such as cranes and metal crushers. Therefore, it is crucial to avoid catastrophic damage to gears by understanding the crack behaviour. Provided the crack does not propagate into the rim, only minor accidents are likely to happen or else catastrophe may be expected again. Therefore, the study of crack behaviour on stress intensity factor (SIF) with different magnitude of moment was conducted. This study implemented the application of extended finite element method (XFEM) in ABAQUS to overcome the limitations of a conventional method, the finite element method (FEM). The need of re-meshing was avoided in this simulation. The crack propagation pathways were visualised using the 'STATUSXFEM'.

Keywords: crack propagation; stress intensity factor; XFEM; gear; moment; contact stress; FEM; AGMA; Hertzian

Reference to this paper should be made as follows: Hiung, F.Z., Al-Qrimli, H.F. and Morris, K.I. (2017) 'Implementation of XFEM in the study of gear crack propagation behaviour using the SIF on different moments', *Int. J. Simulation and Process Modelling*, Vol. 12, Nos. 3/4, pp.362–368.

Biographical notes: Fung Zen Hiung is a graduate of Bachelor of Mechanical Engineering in Curtin University Sarawak Campus. He was awarded the letter of commendation twice from Curtin University Sarawak for obtained average of 75% and above. His research interests include modelling/simulation, robotics and automation.

Haidar F. Al-Qrimli holds a BSc, MSc and PhD in Mechanical Engineering. He obtained his PhD from The University of Nottingham, majoring in applied mechanics with specific research focus on composite materials and robotics. He was a top ten candidate in his undergraduate as well as in postgraduate studies. He received a full scholarship in his PhD, awarded to excellent students in recognition for their achievements. He is holding a patent in Malaysia with title: A hybrid serial-parallel-parallel robotic arm, Patent No. PI 2012002538, Malaysia. He is an active researcher who has published numerous research papers and journal articles within his fields of interest. He is a full member of the British Institute of Mechanical Engineers (IMechE) and is a Chartered Engineer (CEng) in the UK.

1 Introduction

According to Xu (2008), in any industrial practices, 74% of gears used are spur gears, 15% are helical gears, 5% are worm gear, 4% are bevel gears and the others are epicycle or internal gears. Therefore, failure due to crack in a spur gear is common. Crack is defined as the opening created when surfaces move in opposite directions. The major causes of crack propagation are mainly due to the magnitude and direction of load and its loading cycle. These factors contribute to a different pattern of crack propagation either through the tooth or towards the rim. According to de Oliveira (2013), when the crack grows toward the rim, it possibly causes catastrophic damage to the gear, causing the machine to stop running. Therefore, it is significantly important to study the behaviour of crack propagation in the gear. Through understandings of crack growth behaviours after crack initiation, engineers are able to design proper safety precautions and maintenance schedules.

Crack initiation occurs at the point that experiences the largest stress (Pandya and Parey, 2013a). Ahamed et al. (2014) and Eriki et al. (2012) also predicted that the crack is initiated at the tooth or specifically below the pitch line. The outcomes of their studies enhanced their prediction on crack initiation through the propagation path along the tooth. Crack propagation is highly dependent on the thickness of rim and the crack position (Curà et al., 2014). He studied the crack propagation for different positions of crack and concluded that as the position changes, the crack propagation path changes for a thin rim gear. On the other hand, Pandya and Parey (2013b) studied the crack propagation at different positions. Lewicki (2001) and Podrug and Jelaska (2006) also studied on spur gear crack propagation with various speed on different backup ratio and different locations respectively. However, both the studies lack information about the stress intensity factor on the crack tip. In contrast, Lewicki et al. (2001) studied the stress intensity factor on effect of different load dynamically on a spiral-bevel gear. By understanding the progress of available researches, the knowledge of stress intensity factor on the crack tip of a spur gear with different magnitudes of torque is unavailable. There is too much focus on a dynamically applied load, neglecting the significance of static load, as there are many applications involving high static load which include different types of cranes and car crushers. Hence, the crack propagation pathway when different magnitudes of moment are applied at a risky position is studied. By observing only the crack propagation pathway, it is insufficient in the design process due to the unavailability of theoretical guidance. Therefore, the stress intensity factor (SIF) at the crack tip is studied to indicate the behaviour of crack propagation towards the remote stress applied, especially on the strength of the cracked gear tooth.

In recent years, finite element method has contributed significant amount of solutions for problems related to crack analysis. However, application of FEM remains challenging in the study of crack propagation. The primary problem in crack growth simulation is the computation of state stress in a cracked body while dealing with the discontinuities in certain fracture criterion (Bordas, 2003). Therefore, extended finite element method (XFEM) is used to overcome the singularity, $1/\sqrt{r}$ problems at the crack tip by incorporating the singularities in local approximation (Edke, 2009). Finite element method has disadvantage in mesh generation as it consumes time and high computer memory capacity. The mesh must be consistent with the discontinuity (Abdelrahman, 2011). In other words, the mesh must be aligned with the domain boundaries. A study by Eriki et al. (2012) on the crack propagation of a spur gear using FEM has used the 'delete and fill' method for re-meshing purposes. This process is tedious and has become a primary problem on dealing with growing cracks. Therefore, XFEM has become a popular alternative in crack propagation analysis. XFEM is independent of the crack as it is able to avoid mesh refinement procedure and can be modelled on fixed mesh (Abdelrahman, 2011). It is because XFEM allows crack to pass through an element. Therefore, application of XFEM is used in this study to visualise and study the behaviour of crack propagation. This method is able to prevent singularities of crack, reduce computational burden and avoid the mesh refinement for every crack growth process.

2 Background

Stress intensity factor is a parameter that describes the cracks' behaviour (Hernandez, 2013). It is generally denoted by K and is described as the stress state at the crack tip region and the resistance of the material. The relation of stress intensity factor and the affecting parameters are shown in equation (1) (Abdelrahman, 2011).

$$K = C\sigma\sqrt{\pi a} \tag{1}$$

where

a length of crack

σ remote stress applied

C finite geometry correction factor.

3 Methodology

3.1 Model generation

Generally for heavy industries, gears with a large module are used due their ability to transmit high load. Therefore, a pair of module 8 gears was selected from the study by Hwang et al. (2013). The specifications of the chosen spur gear model are shown in Table 1. The gear models were generated using Solidworks and was then extruded into smaller parts to reduce simulation the time. The gear model was then imported to ABAQUS for simulation setting up.

The gear pair was adjusted so that both surfaces of pitch circle of the gear teeth touch each other for loading transfer. The material property of the gear was defined E = 200 Gpa and ν = 0.3. Friction factor of 0.2 was included as

mentioned by Xu (2008) where frictions must be considered as long as two surfaces are in contact. Since it was a static analysis, the outer surfaces of the pinion including the shaft surface were fixed. For a pinion, the gear was made to rotate at a reference point with applied moment.

Table 1 Specifications of spur gear

Parameter	*Pinion and gear*
Number of teeth, N	22
Module, m	8
Pitch diameter, D (mm)	176
Base diameter, D_b (mm)	165.39
Pressure angle, ∅	20°
Face width, w	120 mm

For a gear tooth in contact, the crucial part of the gear is at the tooth surfaces which are in contact. Therefore, the contact edges were meshed with very high density of 0.1 mm mesh size. According to Xu (2008), a hexahedron element has higher simulation precision than a tetrahedron. Therefore, hex typed element was used in this model as shown in Figure 1.

Figure 1 Meshed gear and pinion (see online version for colours)

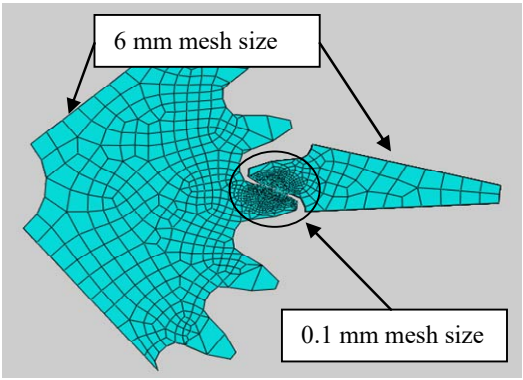

3.2 Model validation

The contact theory was used in the model validation. The theory allows the observation of the deformation of mechanisms that are in contact (Abdelrhman et al., 2016). The contact stress was generated in ABAQUS using the finite element method by applying five different magnitudes of torque on the gear. For validation purposes, the ABAQUS simulated contact stress is then compared to the calculated theoretical Hertzian and AGMA contact stress. The equations are shown in equations (2) and (3) whereas the values for respective parameters are shown in Tables 2 and 3.

By referring to Gupta et al. (2012)

$$p_{c\max} = \frac{4F}{BL\pi} \tag{2}$$

$$B = \sqrt{\frac{8F}{\pi W}\frac{\frac{1-\nu_p{}^2}{E_p}+\frac{1-\nu_g{}^2}{E_g}}{\frac{1}{D_p}+\frac{1}{D_g}}} \tag{3}$$

Given that,

Table 2 Percentage difference of contact stress

Parameter	*Descriptions*	*Value*
D_g and D_p	Pitch diameter of gear and pinion respectively	176 mm
E_g and E_p	Young's modulus of gear and pinion respectively	200 MPa
F	Resultant force	24,028.65 N
p_c	Hertzian contact stress	398.92 MPa
v_g and v_p	Poisson ratio of gear and pinion respectively	0.3
W	Face width	120 mm

By referring to Association (1995)

$$\sigma_H = Z_E\sqrt{F_t K_o K_v K_s \frac{K_h}{2RWZ_I}} \tag{4}$$

Given that,

Table 3 Percentage difference of contact stress

Parameter	*Descriptions*	*Value*
σ_H	AGMA contact stress	402.71 mm
F_t	Tangential force	22,579.55 N
K_h	Load distribution factor	1
K_o	Overload factor	1
K_v	Dynamic factor	1
K_s	Size factor	1
R	Pitch radius	88 mm
W	Face width	120 mm
Z_E	Elastic coefficient	187
Z_I	Geometry factor for pitting resistance	0.22

Since contact stress occurs at the point of contact, the highest stress was seen at the point of the surface contact between the tooth of gear and pinion as shown in Figure 2. The contact stress along the tooth is also compared with previous outcome as shown in Figure 3. Table 4 summaries the percentage difference between the simulated and theoretical contact stress.

Figure 2 Contact stress at the surface of the gear (see online version for colours)

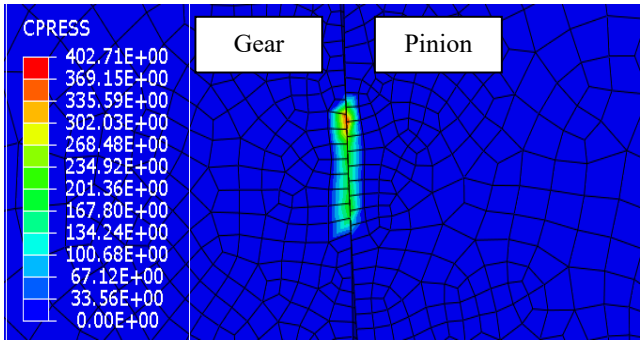

Figure 3 Contact stress along the gear tooth from (a) current simulation and (b) Wright (2013) (see online version for colours)

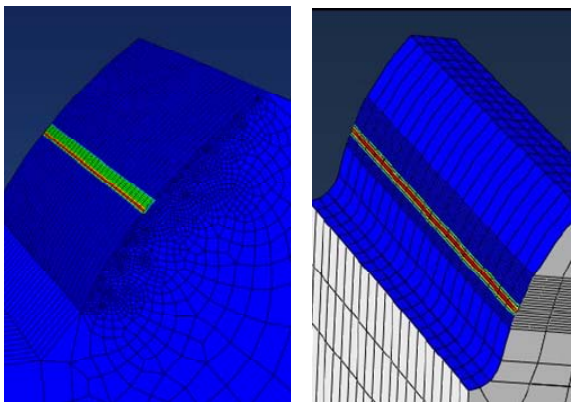

(a) (b)

Table 4 Percentage difference of contact stress

Torque (MN.mm)	1.987
ABAQUS (MPa)	402.71
Hertzian (Mpa)	398.98
Percentage error (%)	0.93
AGMA (Mpa)	412.23
Percentage error (%)	2.31

3.3 Crack initiation

Figure 4 shows two different crack positions which were used for validation and analysis purposes. The location of crack on the fillet used for validation has been used in the study by Ahamed et al. (2014) and Wright (2013). It is due to the higher stress distribution at the particular area. The position below the midpoint of fillet is likely to be more dangerous due to the chance of growing towards the rim. However, Position E which is indicated in the study by Curà et al. (2014) was not used because it is located relatively far from the concentrated stress area. Therefore, only Position D was used for analysis purposes.

According to Pandya and Parey (2013a), for a contact ratio less than 2, the shape of the crack must be curve. In this study, the contact ratio of the model was calculated as 1.58 and therefore the crack is curved in shape. As simplification, only the crack length of 10% was used as it is more likely to happen in practice. The 10% of crack length can be found in the study by Pandya and Parey (2013b). The cracks can be visualised in Figure 4.

Figure 4 Location of crack for validation and analysis (see online version for colours)

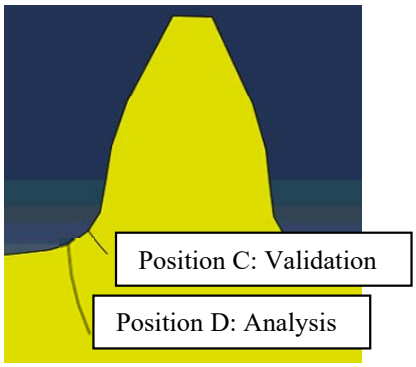

The crack and the enrichment region were defined using ABAQUS. The enrichment region is the region where a crack is initiated and subsequently grows. Then, the material properties of the crack were defined in the damage for traction separation law and damage evolution as shown in Table 5.

Table 5 Material properties for damage criteria

Properties	*Value*
Maximum principal stress	472 MPa
Fracture toughness	65 MPa.$\sqrt{\text{mm}}$
Fracture energy	21.125 mJ/mm^2

For validation purposes, a moment of 50 MN.mm was applied to the gear tooth. It is because when the largest moment is applied on the gear, it shows the most significant crack propagation pathway. For analysis purposes, moments from 10 MN.mm to 50 MN.mm were applied to study the behaviour of crack propagation on the stress intensity factor when different magnitude is applied. The moment applied on the gear is visualised in Figure 5.

Figure 5 Direction of moment applied on gear (see online version for colours)

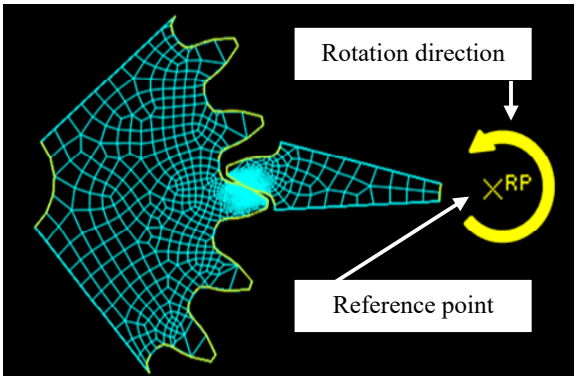

Figure 6 Mesh partition, (a) before and (b) after mesh (see online version for colours)

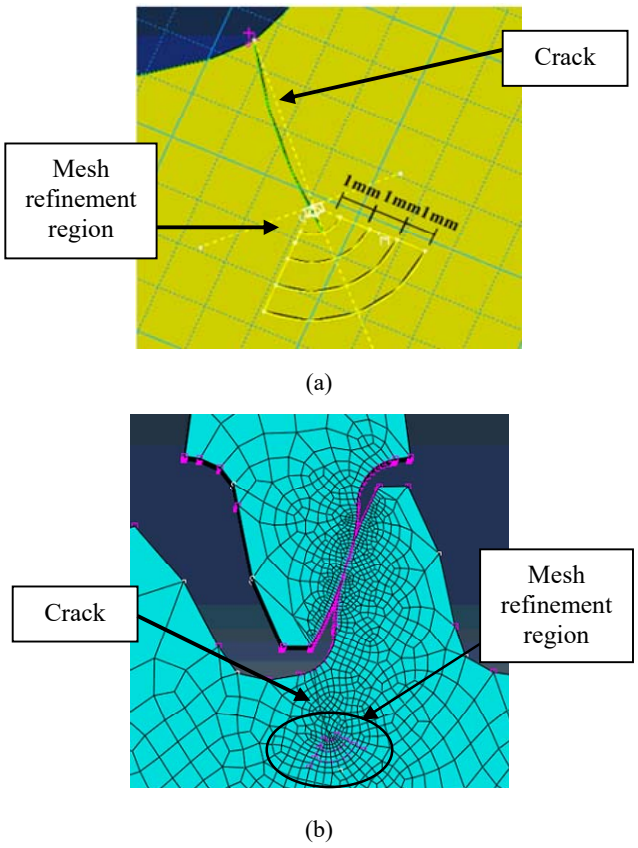

3.4 Mesh generation

In the XFEM, the crack will elongate in a certain distance away from the crack initiation point. Therefore, a new mesh region of the crack with higher density was defined to allow the crack to propagate accurately through the region. A quarter circular arc region with a centre point at the initial crack point was created perpendicular to the crack. The arc was then offset with a distance of 1 mm for each interval, as described in Figure 6. The main motivation of using the particular pattern for the mesh region is to avoid high density of mesh region of the predicted crack path area. The area is estimated to provide the maximum limits of the crack growth direction by assuming horizontal and vertical crack growth. In total, 28,840 elements were generated which is fewer than the software limitation of 100,000 nodes.

3.4 Crack validation

Crack was defined by ABAQUS at the gear tooth. However, it might not behave in a proper way. Therefore, to ensure that the crack is able to react properly accordingly to the force applied towards the gear, the crack propagation of a typical position which is shown in Figure 7 was used to compare with the previous studies.

The gear was applied with a moment of 50 MN.mm and was allowed to crack. The purpose to use a large magnitude of moment is to ensure a better visualisation with longer crack. From Figure 7, it can be clearly shown that the crack grows towards the end of the gear fillet along the gear tooth. Figure 7 also shows the same crack propagation pathway in comparison to previous crack propagation. By comparing both crack propagation pathways, it can be concluded that the crack shows the crack properties where the crack will grow when the load applied exceeds the maximum limits of the material properties. Therefore, the crack in the gear was validated.

Figure 7 Crack propagation path by (a) Molatefi et al. (2015), (b) Curà et al. (2016) and (c) current simulation from ABAQUS (see online version for colours)

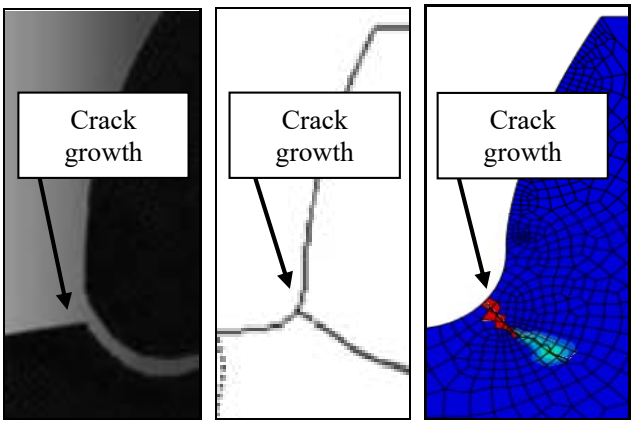

4 Results and discussion

4.1 Crack propagation

Crack propagation pathway was visualised using 'STATUSXFEM' in ABAQUS. The pathway is shown in Table 6. The contour with red colour region indicates the initial crack whereas the other colours indicate the growth.

From Table 6, it is seen that there is no crack growth when moment of 10 MN.mm is applied. It can be also observed that the crack propagates in the same path regardless of the magnitude of moment is applied. The consistency in crack growth direction for different magnitudes of moment is due to the same direction of resultant force is acting on the gear tooth surface. Therefore, it can be concluded that the magnitude of moment applied is independent of the crack growth pathway.

Since the crack grows independently of the applied moment, the predicted crack growth will be along the body of the gear. It will not grow towards the rim which will lead to catastrophic accidents. The usage of the gear in practice is still allowable unless the crack grows nearer to the fillet or any end point. It is because as the crack tip is nearer to its end point or fillet, the structure of the gear is weakened. Therefore, to prevent any life threatening incidents by considering the economic benefits, the gear is considered safe to be used unless the crack tip reaches a point near to the tip's endpoint.

Table 6 Crack propagation path of different moment (see online version for colours)

Moment (MN.mm)	*Crack propagation pathway*	*Odb*
10	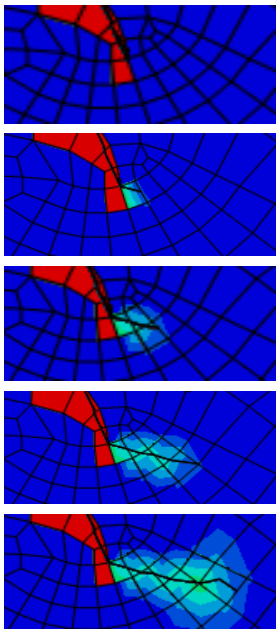	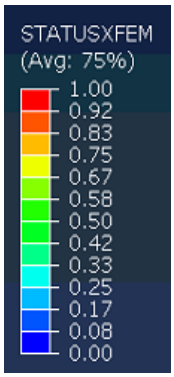
20		
30		
40		
50		

4.2 *Stress intensity factor*

Stress intensity factor describes the behaviour of crack or the state stress at the tip. Generally, the larger the magnitude of the moment, the larger the stress intensity factor. Eventually, the SIF will exceed the fracture toughness or is known as critical stress intensity factor and the crack will grow. The stress intensity factor along the tooth for different moments was obtained from ABAQUS by requesting the output of SIF. The values of SIF outputs from ABAQUS are accordingly to the nodes along the crack tip. Since there are 20 elements along the crack tip, there are 21 nodal solutions of stress intensity factor. The results are shown in Figures 8 and 9 for Mode I and Mode II respectively.

Figure 8 Graph of SIF against node number for Mode I (see online version for colours)

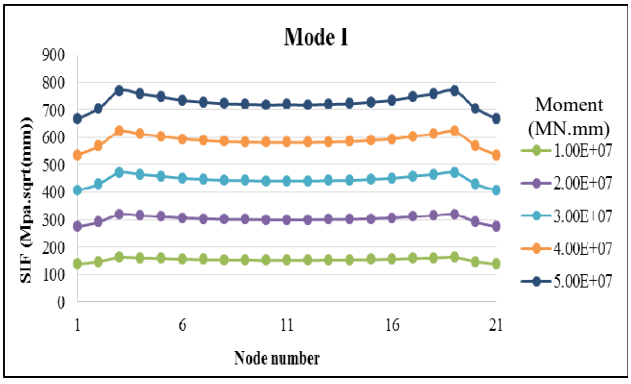

Figures 8 and 9 show that the curves are less deviated as the moment applied reduces. It is mainly due to the impact dealt on the gear. In a step time of 1 s, a total amount of 50 MN.mm moment applied to a gear will have a higher impact in comparison to the impact dealt by a moment of 10 MN.mm. The high impact causes the instability of stress distribution along the tooth because the gear has lesser time to distribute the stress. The different magnitude of stress along the tooth causes the crack to grow unevenly along the tooth. For a condition with a moment of 10 MN.mm, the stresses are able to distribute more evenly along the crack. Therefore, the crack will grow at a stable rate and leads to an even SIF along the tooth.

Figure 9 Graph of SIF against node number for Mode II (see online version for colours)

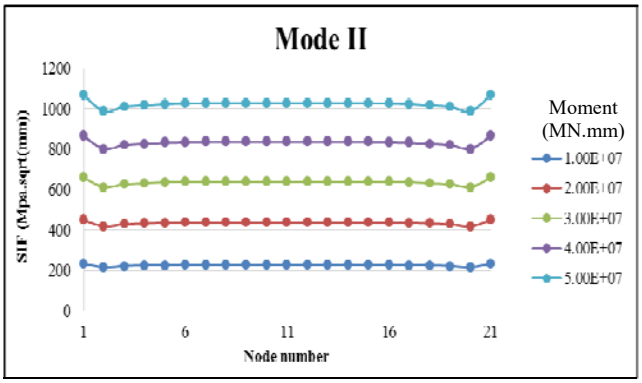

It can be seen that KII is the dominant mode in crack growth. Since KII is more than KI, there is more in-plane shear compared to tearing. It is because the directions of crack and force are similar. Eventually, it causes a significant compressive stress at the crack tip. It results in the increase of tendency to shear compared to tearing.

The positive curves shown in Figure 9 are actually negative values. The curves are made to positive to ease the explanation and description of crack behaviour. The negativity of the SIF is mainly due to the compressive stress that eventually leads to a compressive in-plane shear.

For Mode I, the curves have lower SIF at the surface of the gear when compared to the SIF in the middle of the gear. Unlike other gear models which have thickness less than 50 mm, the gear model used in this simulation has thickness of 120 mm. The thickness of the gear will lead to more stress distributed in the area at middle of the thick spur gear. The higher stress at the crack tip increases the rate of fracture. Since fracture mode I involves force normal to the plane, the tendency to tear or to experience tensile opening is more and therefore, it leads to a higher SIF.

For Mode II which describes the in-plane shear stress, the shape of curve is a reflection of Mode I. Unlike Mode I, for Mode II, the stresses experienced at the area in the middle of the gear is lesser compared to the surface of the gear. Since the area experiences less stress, the tendency to experience an in-plane shear is lower. On the other hand, the surface of the gear has the highest SIF. The stress is distributed along the tooth and since the surface of the gear is the weakest, the crack near the surface has a higher in-plane compressive stress compare to the area in the middle.

Therefore, the nodes at the surface of gear have the highest SIF along the tooth.

5 Conclusions

In this study, the behaviour of crack propagation on different magnitude of forces has been investigated using the XFEM. Therefore, the need of remeshing in this study was avoided. The behaviour of crack was analysed using the stress intensity factor for Mode I and Mode II. Through data analysis and crack propagation visualisation, the objectives of the study were achieved and the outcomes of the study are listed below.

1 The value of SIF of mode II is more than that of mode I for a crack at the position. This is because there is more in-plane shear than tearing.

2 The tendency to tear or to experience tensile opening is more in the middle of the gear. The crack near the surface has a higher in-plane compressive fracture mode compared to the area in the middle.

3 The crack growth is visualised using the 'STATUSXFEM' by applying the XFEM which indicates the presence of the crack. It shows that the growth of crack is independent of the moment applied.

Further investigation can be done to improve the impact of the results. In this study, the crack is studied as a static gear. For further study, the gear can be analysed dynamically where the gear is made rotating to determine the fatigue life of a cracked gear model. Better prediction can be obtained by understanding the maximum number of rotations that the gear can last.

References

Abdelrahman, M. (2011) *Modeling Multiple Crack Propagation in Brittle Materials using the Extended Finite Element*, Master of Science in Civil Engineer, University of Colorado at Boulder, CO.

Abdelrhman, A.M., Al-Qrimli, H.F., Hadi, H.M., Mohammed, R.K. and Sultan, H.S. (2016) 'Times three dimensional spur gear static contact investigations using finite element method', *Modern Applied Science*, Vol. 10, p.145.

Ahamed, N., Pandya, Y. and Parey, A. (2014) 'Spur gear tooth root crack detection using time synchronous averaging under fluctuating speed', *Measurement*, Vol. 52, pp.1–11.

Association, A.G.M. (1995) *AGMA 2101-C95: Fundamental Rating Factors and Calculation Methods for Involute Spur and Helical Gears*, Metric version, American Gear Manufacturers Association, Alexandria, VA.

Bordas, S. (2003) *Extended Finite Element and Level Set Methods with Applications to Growth of Cracks and Biofilms*, North Western University.

Curà, F., Mura, A. and Rosso, C. (2014) *Investigation about Crack Propagation Paths in Thin Rim Gears*, Frattura ed Integritá Strutturale, p.446.

de Oliveira, F.X.G.Z. (2013) *Crack Modelling with the eXtended Finite Element Method*, University of Lisbon.

Edke, M.S. (2009) *Shape Design Sensitivity Analysis and Optimization for 2-D Structural Components under Mixed-mode Fracture using Extended Finite Element Method and Level Set Method*, University of Oklahoma.

Eriki, A.K., Ravichandra, R. and Mustaffa, M.E. (2012) 'Spur gear crack propagation path analysis using finite element method', *International Multi Conference of Engineers and Computer Scientists*, Hong Kong.

Gupta, M.B., Choubey, M.A. and Varde, M.G.V. (2012) 'Contact stress analysis of spur gear', *International Journal of Engineering Research and Technology*, ESRSA Publications.

Hernandez, L.A. (2013) Assessment of ABAQUS capabilities for crack growth and calculation of energy release rate. The University of Texas at El Paso.

Hwang, S-C., Lee, J-H., Lee, D-H., Han, S-H. and Lee, K-H. (2013) 'Contact stress analysis for a pair of mating gears', *Mathematical and Computer Modelling*, Vol. 57, pp.40–49.

Lewicki, D.G. (2001) *Effect of Speed (Centrifugal Load) on Gear Crack Propagation Direction*, DTIC Document.

Lewicki, D.G., Handschuh, R.F., Spievak, L.E., Wawrzynek, P.A. and Ingraffea, A.R. (2001) 'Consideration of moving tooth load in gear crack propagation predictions'.

Pandya, Y. and Parey, A. (2013a) 'Failure path based modified gear mesh stiffness for spur gear pair with tooth root crack', *Engineering Failure Analysis*, Vol. 27, pp.286–296.

Pandya, Y. and Parey, A. (2013b) 'Simulation of crack propagation in spur gear tooth for different gear parameter and its influence on mesh stiffness', *Engineering Failure Analysis*, Vol. 30, pp.124–137.

Podrug, S. and Jelaska, D. (2006) 'Influence of different gear load models on crack propagation predictions', *DS 36: Proceedings DESIGN 2006, the 9th International Design Conference*, Dubrovnik, Croatia.

Wright, A. (2013) *A Comparison of the Tooth-Root Stress and Contact Stress of an Involute Spur Gear Mesh as Calculated by FEM and AGMA Standards*, Rensselaer Polytechnic Institute.

Xu, R. (2008) *Finite Element Modeling and Simulation on the Quenching Effect for Spur Gear Design Optimization*, The University of Akron.